Available online at www.sciencedirect.com
SCIENCE DIRECT®
ELSEVIER
Journal of Sound and Vibration 289 (2006) 952–966
JOURNAL OF SOUND AND VIBRATION
www.elsevier.com/locate/jsvi

Nonlinear dynamics of a flexible mechanism with impact

Mihai Dupac, Dan B. Marghitu*

Department of Mechanical Engineering, Auburn University, Auburn, AL 36849, USA

Received 29 September 2004; received in revised form 25 February 2005; accepted 1 March 2005
Available online 2 June 2005

Abstract

The nonlinear dynamics of a slider-crank mechanism with a flexible rod is considered in this study. The flexible rod is modeled with lumped masses and periodically impacted by an external flexible sphere. The impact is modeled using a kinematic coefficient of restitution. Nonlinear dynamics tools are applied to analyze the simulated data captured from the connecting rod of the mechanism. The chaotic behavior of the system is analyzed. The stability of the motion is studied using the Lyapunov exponents. The dependence between the Lyapunov exponents and the corresponding angular velocity of the driver link of the mechanism is investigated.

1. Introduction

The effect of impact and flexibility on the dynamic behavior of mechanical systems has been the subject of numerous investigations. Their practical significance is considerable when high precision, alignment, clearances are important. Impact is the most common type of dynamic conditions that gives rise to impulsive force which affects the vibrational characteristic of the mechanical system.

The impact responses of a multi-body system with lumped mass was studied by Khulief and Shabana [1]. A study approach in longitudinal collision problems for some simple structural

*Corresponding author. Tel.: +1 334 844 3335; fax: +1 334 844 3307.
E-mail address: marghitu@eng.auburn.edu (D.B. Marghitu).

0022-460X/$ - see front matter
doi:10.1016/j.jsv.2005.03.002

systems modeled by a series of rods and rigid elements has been realized by Mioduchowski et al. [2]. The design and control of some impact systems have been analyzed in Rattan and Brown [3], the design and dynamics was studied in Rubinstein [4].

The problem of reducing the chaotic response of a simple mechanical system in the continuous case was studied by Shaw and Rand [5]. Systems with non-ideal elements such as clearance connections have been found to exhibit chaotic behavior; Moon and Shaw [6], Shaw [7]. Dubowsky and Moening [8] investigated the impact responses in a constrained mechanical system with flexible components as part of the study of dynamics of mechanical systems with clearances. Moreover, it has been found experimentally and analytically, that subharmonic and chaotic vibrations can appear under periodic excitation; Moore and Shaw [9], Shaw et al. [10].

Chaotic behavior in four-bar mechanisms and slider-crank mechanisms with joint clearances has been studied in Refs. [11,12]. Non-periodic and sensitive to initial conditions responses have been found in these studies.

Szuminski and Kapitaniak [13] studied the stability regions of periodic trajectories of the manipulator motion. The responses indicate that chaotic behavior occurs under certain conditions.

Two methods of formulation (algebraic and differential), were used to develop the necessary equations to solve impact problems. The coefficient of restitution was used to derive a relation between the normal components of the approach and departure velocities at the contact point. The latter method divides the collision period into the compression and restitution phases. Poisson's hypothesis defines a kinetic quantity that relates the normal impulses at the contact point that occur during each phase. The approaches also evolved differently in the treatment of the motion in the tangential direction at the point of contact.

A comprehensive analysis of the theoretical outcomes that are predicted by each method using different definitions of the coefficient of restitution can be found in Ref. [14].

Marghitu and Hurmuzlu [14], uses coupled axial and transverse elastic deformations to study the collisions as well as frictional effects at the impacting point for different impact angles. The influence of axial waves are not so important in the case of oblique impact. The main influence for this kind of impact is the transverse vibrations and that is why we neglected the axial waves.

In this paper the nonlinear dynamics of a slider-crank mechanism with flexible rod and impact is studied. The flexible link is periodically impacted by the same external elastic sphere. In the impact moment the sphere is in un-deformed state. The time period between two successive impacts represents the required time for a complete revolution of the rigid driver link. The flexible rod is modeled as n successive equal rigid rods connected with torsional springs. The elastic sphere is modeled as a mechanical system with lumped masses, springs, and rigid massless rods (Ref. [15]). The kinematic coefficient of restitution is used to study the impact of the system. The algebraic impact equations with friction and a kinematic coefficient of restitution gives the best results for our case (Ref. [14]). The generalized equations are formulated and solved for the motion of the system with periodic impact. Nonlinear dynamics tools are applied to analyze the simulated data captured from the connecting rod of the mechanism. The stability of the motion is studied using the Lyapunov exponents. The dependence between the Lyapunov exponents and the corresponding angular velocity is investigated. This study is different from the others because of the modeling of the mechanical system and nonlinear analysis.

2. System model

2.1. Flexible link

For the study of the slider-crank mechanism, the model shown in Fig. 1 is proposed. The planar mechanism is modeled as a mechanical system with $n+1$ rigid rods. A fixed reference frame xOy is chosen.

In Fig. 1 the rod A_1A_2 (the link 1) is rigid. The connecting rod A_2A_{n+1} is modeled using n successive equal rigid rods (links $2, 3, \ldots, n+1$) connected with torsional springs (with spring constants k_t). The rigid slider C is the link $n+2$. The rod 1 has length L_1 and is linked to rod 2 with a pin-joint. Each one of the rods $2, 3, \ldots, n+1$ has the mass m, moment of inertia J and length $l = L_2/n$. The distance L_2 is the distance A_2A_{n+1} when the flexible link is not deformed. The rod $n+1$ is linked to the slider $n+2$ with a pin-joint. The spring constants are denoted by k_t.

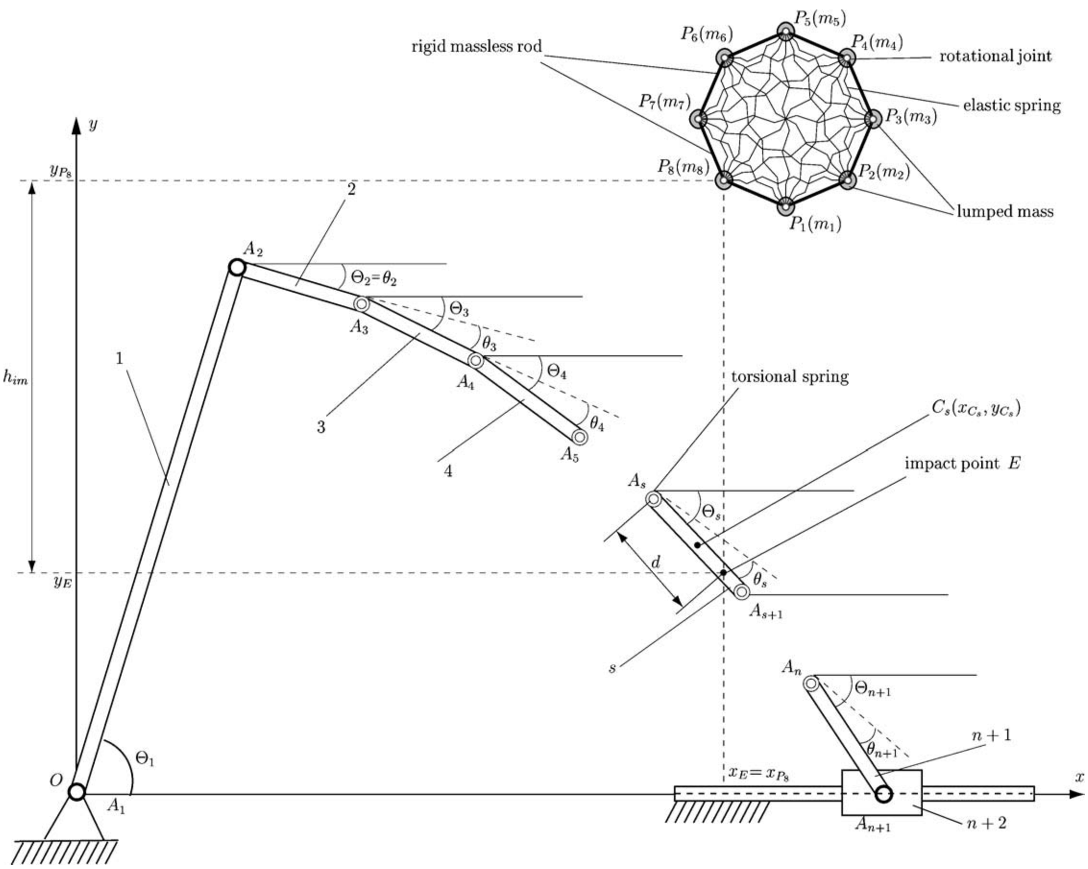

Fig. 1. Mechanical model of the slider-crank mechanism with the rigid link A_1A_2, the connecting rod A_2A_{n+1} modeled using n successive equal rigid rods A_2A_3, A_3A_4, $A_4A_5, \ldots, A_sA_{s+1}, \ldots, A_nA_{n+1}$, the angles Θ_1, Θ_2, Θ_3, $\Theta_4, \ldots, \Theta_s, \ldots, \Theta_{n+1}$ between the corresponding links and the Ox axis, the relative angles θ_1, θ_2, θ_3, $\theta_4, \ldots, \theta_s, \ldots, \theta_{n+1}$, and the flexible droplet with the particles $P_1(m_1)$, $P_2(m_2), \ldots, P_8(m_8)$.

For the slider-crank mechanism shown in Fig. 1, x_{C_i} and y_{C_i} represent the coordinates of the mass center of the rod i (for $i = 1, \ldots, n+1$), x_{A_i} and y_{A_i} the coordinates of the node point A_i, θ_i the relative angle between rod i and rod $i+1$ (for $i = 2, \ldots, n$), and Θ_i the absolute angle between the horizontal direction and rod i (for $i = 1, \ldots, n+1$).

At the beginning of the rotational motion of the slider-crank mechanism, the flexible link is in undeformed state, that is, the rods $2, 3, \ldots, n+1$ are located along a straight line and $A_2A_{n+1} = L_2$.

One can define the position of each link $i = 1, 2, \ldots, n+2$ using the length L_1 of link 1, the lengths l of each link $i = 2, \ldots, n+1$ and the angles Θ_i between the links $i = 1, \ldots, n+1$ and the Ox axis.

The absolute angle Θ_i of rod $i = 2, \ldots, n+1$ is the summation of the relative angles θ_j ($j = 2, \ldots, i$), as described in Fig. 1

$$\Theta_i = \sum_{j=2}^{i} \theta_j \quad \text{for } i = 2, \ldots, n+1.$$

The system of two successive rods i and $i+1$ is shown in Fig. 2.

For the slider-crank mechanism, the position vector of the center of the mass C_i of the link $i = 1, 2, \ldots, n+2$ is given by $\mathbf{r}_{C_i} = x_{C_i} = x_{C_i}\mathbf{i} + y_{C_i}\mathbf{j}$.

The horizontal and the vertical coordinates of the mass center of the rod $i = 2, \ldots, n+1$ are

$$x_{C_i} = x_{A_2} + l \sum_{j=2}^{i} \left(1 - \frac{\delta_i^j}{2}\right) \cos \Theta_j, \quad y_{C_i} = y_{A_2} - l \sum_{j=2}^{i} \left(1 - \frac{\delta_i^j}{2}\right) \sin \Theta_j,$$

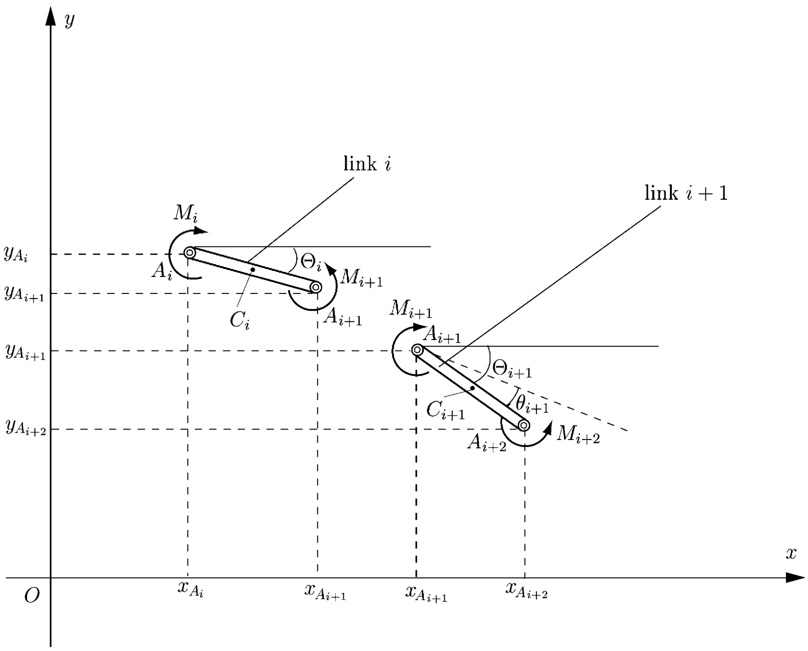

Fig. 2. System of two successive rods, link i and $i+1$ with C_i and C_{i+1} the corresponding mass center for each link, with the angles Θ_{i+1} and θ_{i+1}, and the moments M_i, M_{i+1}, M_{i+2} at the corresponding node A_i, A_{i+1}, A_{i+2}.

where

$$\delta_i^j = \begin{cases} 1 & \text{if } i = j \\ 0 & \text{if } i \neq j \end{cases}, \quad x_{A_2} = L_1 \cos \Theta_1 \quad \text{and} \quad y_{A_2} = L_1 \sin \Theta_1.$$

The center of the mass position of the link $i = n + 2$ (slider C) is given by

$$x_{C_{n+2}} = L_1 \cos \Theta_1 + l \sum_{j=2}^{n+1} \cos \Theta_j, \quad y_{C_{n+2}} = L_1 \sin \Theta_1 - l \sum_{j=2}^{n+1} \sin \Theta_j.$$

2.2. Equation of motion

The velocity vector of C_i is the derivative with respect to time of the position vector of C_i for $i = 1, 2, \ldots, n + 2$ and is given by $\mathbf{v}_{C_i} = \dot{\mathbf{r}}_{C_i} = \dot{x}_{C_i}\mathbf{i} + \dot{y}_{C_i}\mathbf{j}$.

The center of the mass velocity for the link $i = 1$ of the mechanism is given by

$$\dot{x}_{C_1} = -\frac{L_1}{2}\dot{\Theta}_1 \sin \Theta_1, \quad \dot{y}_{C_1} = \frac{L_1}{2}\dot{\Theta}_1 \cos \Theta_1.$$

The centers of the mass velocity for the links $i = 2, \ldots, n + 1$ are

$$\dot{x}_{C_i} = -L_1\dot{\Theta}_1 \sin \Theta_1 - l \sum_{j=2}^{i} \left(1 - \frac{\delta_i^j}{2}\right)\dot{\Theta}_j \sin \Theta_j,$$

$$\dot{y}_{C_i} = L_1\dot{\Theta}_1 \cos \Theta_1 - l \sum_{j=2}^{i} \left(1 - \frac{\delta_i^j}{2}\right)\dot{\Theta}_j \cos \Theta_j.$$

The center of the mass velocity for the link $i = n + 2$ (slider C) of the mechanism is given by

$$\dot{x}_{C_{n+2}} = -L_1\dot{\Theta}_1 \sin \Theta_1 - l \sum_{j=2}^{n+1} \dot{\Theta}_j \sin \Theta_j \quad \dot{y}_{C_{n+2}} = 0.$$

The acceleration vector of C_i is the double derivative with respect to time of the position vector of C_i for $i = 1, 2, \ldots, n + 2$, that is, $\mathbf{a}_{C_i} = \ddot{\mathbf{r}}_{C_i} = \ddot{x}_{C_i}\mathbf{i} + \ddot{y}_{C_i}\mathbf{j}$.

The centers of the mass acceleration for the link $i = 1$ is

$$\ddot{x}_{C_1} = -\frac{L_1}{2}\ddot{\Theta}_1 \sin \Theta_1 - \frac{L_1}{2}\dot{\Theta}_1^2 \cos \Theta_1, \quad \ddot{y}_{C_1} = \frac{L_1}{2}\ddot{\Theta}_1 \cos \Theta_1 - \frac{L_1}{2}\dot{\Theta}_1^2 \sin \Theta_1.$$

The center of the mass acceleration for the links $i = 2, \ldots, n + 1$ are given by

$$\begin{aligned} \ddot{x}_{C_i} = & -L_1\ddot{\Theta}_1 \sin \Theta_1 - L_1\dot{\Theta}_1^2 \cos \Theta_1 \\ & - l \sum_{j=2}^{i} \left(1 - \frac{\delta_i^j}{2}\right)\ddot{\Theta}_j \sin \Theta_j - l \sum_{j=2}^{i} \left(1 - \frac{\delta_i^j}{2}\right)\dot{\Theta}_j^2 \cos \Theta_j, \end{aligned}$$

$$\ddot{y}_{C_i} = L_1\ddot{\Theta}_1 \cos \Theta_1 - L_1\dot{\Theta}_1^2 \sin \Theta_1 \\ - l \sum_{j=2}^{i} \left(1 - \frac{\delta_i^j}{2}\right) \ddot{\Theta}_j \cos \Theta_j + l \sum_{j=2}^{i} \left(1 - \frac{\delta_i^j}{2}\right) \dot{\Theta}_j^2 \sin \Theta_j.$$

The center of the mass acceleration for the slider C is given by

$$\ddot{x}_{C_3} = -L_1\ddot{\Theta}_1 \sin \Theta_1 - L_1\dot{\Theta}_1^2 \cos \Theta_1 - l \sum_{j=2}^{n+1} \ddot{\Theta}_j \sin \Theta_j - l \sum_{j=2}^{n+1} \dot{\Theta}_j^2 \cos \Theta_j,\ \ddot{y}_{C_3} = 0.$$

One can write the Lagrange differential equation of motion with no impact for the slider-crank mechanism

$$\frac{\mathrm{d}}{\mathrm{d}t}\left(\frac{\partial T_{\mathrm{sc}}}{\partial \dot{q}_i}\right) - \frac{\partial T_{\mathrm{sc}}}{\partial q_i} = Q_i \quad \text{for } i = 1, 2, \ldots, n,$$

where T_{sc} is the total kinetic energy of the system, Q_i are the generalized forces and $q_i = \Theta_i,\ i = 1, \ldots, n+1$, are the generalized coordinates.

The total kinetic energy is $T_{\mathrm{sc}} = \sum_{i=1}^{n+2} T_i$, where the kinetic energy for each link $i = 1, 2, \ldots, n+2$ is $T_i = \frac{1}{2} m_i \mathbf{v}_{C_i}^2 + \frac{1}{2} I_{C_i} \boldsymbol{\omega}_i^2$. The angular velocity vectors of the links $i = 1, 2, \ldots, n+1$ are $\boldsymbol{\omega}_i = \dot{\Theta}_i \mathbf{k}$.

The elastic moment for the ith ($i = 2, \ldots, n$) link is $M_i = -k_t \theta_i$.

The spring constant is computed using $k_t = EJ/nl$, where E is Young's modulus [4]. Stoianovici and Hurmuzlu [16] used a similar discrete model with springs and the model was verified with experimental data. One can conclude that a system with spring constants calculated with the previous formula gives accurate results. Dupac et al. [15] calculated the spring constants for more complicated 3D system.

The generalized forces can be written as

$$Q_1 = \sum_{j=1}^{n+2} \frac{\partial \mathbf{r}_{C_j}}{\partial \Theta_1} \cdot \mathbf{G}_j + \frac{\partial \boldsymbol{\omega}_1}{\partial \dot{\Theta}_1} \cdot \mathbf{M}_1,$$

$$Q_i = \sum_{j=1}^{n+2} \frac{\partial \mathbf{r}_{C_j}}{\partial \Theta_i} \cdot \mathbf{G}_j + \frac{\partial \boldsymbol{\omega}_i}{\partial \dot{\Theta}_i} \cdot (\mathbf{M}_i + \mathbf{M}_{i+1}), \quad i = 2, 3, \ldots, n+1.$$

The gravitational forces acting on the links $i = 1, 2, \ldots, n+1$ are $\mathbf{G}_i = -m_i g \mathbf{j}$, and the motor torque that acts on the link 1 is $\mathbf{M}_1 = M_0(1 - \omega_1/\omega_0)\mathbf{k} = M_0(1 - \dot{\Theta}_1/\omega_0)\mathbf{k}$. For the system of two successive rods i and $i+1$ shown in Fig. 2, M_i represents the moment at node A_i.

2.3. Mechanical model of impacting elastic sphere

The flexible link is periodically impacted by the same external elastic sphere. In the impact moment the elastic sphere is considered in un-deformed state. Suppose that the elastic sphere impacts the flexible link s at the point E. The position vector of the impact point of the elastic sphere with the link s is shown in Fig. 1 and takes the form

$$\mathbf{r}_E = \mathbf{r}_{A_2} + \left(l \sum_{j=2}^{s-1} \cos \Theta_j + d \cos \Theta_s \right)\mathbf{i} - \left(l \sum_{j=2}^{s-1} \sin \Theta_j + d \sin \Theta_s \right)\mathbf{j},$$

where d represents the distance from the point A_s to the impact point E and $d<l$.

The time period between two successive impacts represents the required time for a complete revolution of the rigid driver link. For the study of impact a mechanical model of the impacting sphere shown in Fig. 1 is proposed.

For the general case, there are q particles, P_i, $i = 1, \ldots, q$ in the system. The total mass of the elastic sphere is $M = \sum_{i=1}^{q} m_{P_i}$, where m_{P_i} is the mass of the particle P_i.

A particular model, with 8 lumped masses, is considered (refer to Fig. 1). The particles are connected with linear elastic springs. Rigid massless rods are used for the exterior of the elastic sphere. There are q rods, connected with rotational joints. Each particle P_i is connected with the other particles with $q-3$ identical springs. In our particular case each particle P_i is connected with five identical springs as shown in Fig. 1.

Each particle can move along the x and y axes. The numbers of dof of the system with eight particles is 8. The position vector of the particle P_i is $\mathbf{r}_{P_i} = x_{P_i}\mathbf{i} + y_{P_i}\mathbf{j}$, for $i = 1, 2, \ldots, q$ where x_{P_i} is the x-coordinate and y_{P_i} is the y-coordinate of particle P_i in a fixed reference frame xOy.

One can define the position of each particle P_i, $i = 1, \ldots, q$, (refer to Fig. 3a), using the length P_1P_q, P_iP_{i+1}, $i = 1, 2, \ldots, q-1$, the angle between P_iP_{i+1} and the Ox axis $\gamma_i(t)$, and the initial lengths ξ_1 and ξ_2. One can write

$$x_{P_1} = \xi_1, \quad x_{P_i} = \xi_1 + \sum_{j=1}^{i-1} b \cos \gamma_j,$$
$$y_{P_1} = \xi_2, \quad y_{P_i} = \xi_2 + \sum_{j=1}^{i-1} b \sin \gamma_j, \tag{1}$$

where $i = 1, 2, \ldots, q-1$ and b is the rod length, $P_iP_{i+1} = b = \text{const}$.

There are q constraint equations in the system

$$(x_{P_q} - x_{P_1})^2 + (y_{P_q} - y_{P_1})^2 = (P_qP_1)^2 = b^2 = \text{const},$$
$$(x_{P_{i+1}} - x_{P_i})^2 + (y_{P_{i+1}} - y_{P_i})^2 = (P_iP_{i+1})^2 = b^2 = \text{const}, \tag{2}$$

where $i = 1, 2, \ldots, q-1$.

In Eq. (1), ξ_1 and ξ_2 represent the distances from the Oy respectively Oy axis to the particle P_1. Therefore, x_{P_8} and y_{P_8}, computed using Eq. (1), represent the x- and y-coordinates of the particle P_8 at the moment the sphere is dropped. The impacting point of the sphere is considered to be at the particle P_8.

In Fig. 1, h_{im} represents the distance covered by the sphere to the impact point and y_E is the y-coordinate of the impact point on the flexible link. The time period Δt, required for the sphere to cover the distance h_{im} is the same as the time required by the mechanism to perform a complete

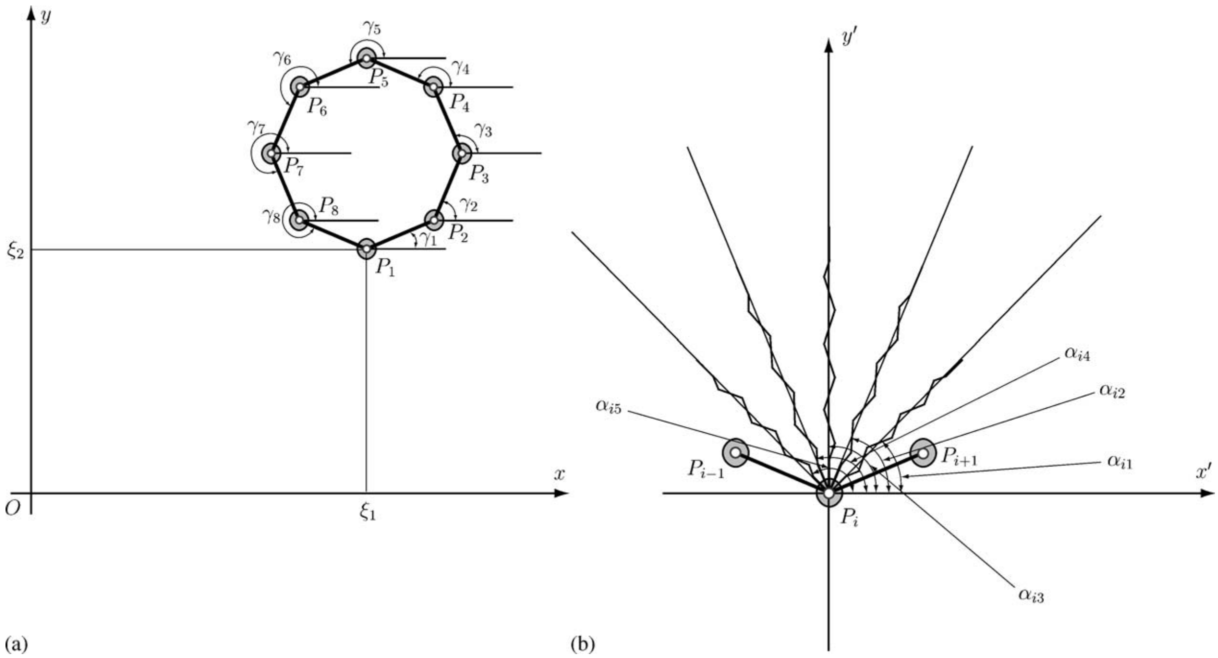

Fig. 3. Spring angles and particles position of the sphere: (a) position of Particle P_i is given using the length P_1P_8, P_iP_{i+1}, $i = 1, 2, \ldots, 7$, the angle $\gamma_i(t)$, and the lengths ξ_1 and ξ_2, (b) spring angles for the configuration P_{i-1}, P_i and P_{i+1} are α_{ij}, $j = 1, 2, \ldots, 5$.

rotation of the rigid driver link. After a time period Δt, the same sphere in un-deformed state, or another identical sphere is dropped from the same position.

Before the impact, the sphere is in a free fall and there are no other external forces except the weight $\mathbf{G} = -Mg\mathbf{j}$, where g is the gravitational acceleration.

Using the positions of the particles P_i, $i = 1, \ldots, q$ one can calculate the spring angles α_{i1}, $\alpha_{i2}, \ldots, \alpha_{in}$ for each particle of the sphere, where α_{ij} represent the angles between the Ox axis and the directions given by P_iP_j (see Fig. 3b for the particular case $q = 8$). Then the elastic force due to each spring is calculated. One can write the expression of the elastic force $\mathbf{F}e_{ij}$ between the particle P_i and P_j as

$$
\begin{aligned}
&\mathbf{F}e_{1j} = k_{1j}\mathrm{d}(P_1P_j)\sin\alpha_{1j}\mathbf{i} + k_{1j}\mathrm{d}(P_1P_j)\cos\alpha_{1j}\mathbf{j}, \quad j = 3, \ldots, q-1,\\
&\mathbf{F}e_{ij} = k_{ij}\mathrm{d}(P_iP_j)\sin\alpha_{ij}\mathbf{i} + k_{ij}\mathrm{d}(P_iP_j)\cos\alpha_{ij}\mathbf{j}, \quad i = 2, \ldots, q-1, \ j = 1, \ldots, q,\\
&\mathbf{F}e_{qj} = k_{qj}\mathrm{d}(P_qP_j)\sin\alpha_{qj}\mathbf{i} + k_{qj}\mathrm{d}(P_qP_j)\cos\alpha_{qj}\mathbf{j}, \quad j = 2, \ldots, q-2,
\end{aligned}
$$

where $\mathrm{d}(P_iP_j)$ denotes the distance between the particle P_i and P_j and k_{ij} represents the elastic constant of the spring between the particles P_i and P_j. In our particular case $k_{ij} = k_s = \text{const.}$ is calculated using [17, p. 226]. Because there are no springs between the particles P_i and P_{i-1}, P_i and P_i, P_i and P_{i+1} one have $j \neq i-1$, $j \neq i$, $j \neq i+1$.

The total elastic force exerted on a particle is the sum of all elastic forces exerted on the particle. One can write the expression of the elastic force exerted on each particle P_i as

$$\begin{aligned}
\mathbf{F}e_1 &= \left(\sum_{l=3}^{q-1} |\mathbf{F}e_{1l}| \sin \alpha_{1l}\right)\mathbf{i} + \left(\sum_{l=3}^{q-1} |\mathbf{F}e_{1l}| \cos \alpha_{1l}\right)\mathbf{j},\\
\mathbf{F}e_i &= \left(\sum_{l=1}^{q} |\mathbf{F}e_{il}| \sin \alpha_{il}\right)\mathbf{i} + \left(\sum_{l=1}^{q} |\mathbf{F}e_{il}| \cos \alpha_{ij}\right)\mathbf{j}, \quad \text{for } i = 2, \ldots, q-1,\\
\mathbf{F}e_q &= \left(\sum_{l=3}^{q-1} \left|\mathbf{F}e_{ql}\right| \sin \alpha_{ql}\right)\mathbf{i} + \left(\sum_{l=3}^{q-1} \left|\mathbf{F}e_{ql}\right| \cos \alpha_{ql}\right)\mathbf{j}.
\end{aligned} \tag{3}$$

Because there are no springs between the particles P_i and P_{i-1}, P_i and P_i, P_i and P_{i+1} one has $l \neq i-1$, $l \neq i$, $l \neq i+1$.

2.4. Equations of motion with impact

One can write the impact differential equation of motion for the slider-crank mechanism as

$$\left(\frac{\partial T_t}{\partial \dot{u}_j}\right)_{t_2} - \left(\frac{\partial T_t}{\partial \dot{u}_j}\right)_{t_1} = R_j,$$

where T_t is the total kinetic energy of the system defined as the sum of the kinetic energy of slider-crank mechanism and the kinetic energy of the elastic sphere, $(\partial T_t/\partial \dot{u}_j)$ are the generalized momenta, R_j are the generalized impulses, $u_j = \Theta_j$ is the generalized coordinate and t_i, $i = 1, 2$ represents the moments of time, respectively before and after the impact.

Considering $\mathbf{R}$ to be the force exerted on the link j by the impacting sphere at the contact point E during the interval time beginning at t_1 and ending at t_2, one can define its components R_x and R_y. One can write

$$\int_{t_1}^{t_2} \mathbf{R}\, \mathrm{d}t = R_x\mathbf{i} + R_y\mathbf{j}.$$

The generalized impulses can be expressed as

$$R_j = \frac{\partial \mathbf{v}_E}{\partial q_j} \int_{t_1}^{t_2} \mathbf{R}\, \mathrm{d}t.$$

Because the generalized velocities are known at the time t_1, when the sphere comes in contact with the flexible link s, it is necessary to find the values of the generalized velocities at the time t_2, the instant at which the sphere loses contact with the flexible link.The velocity of the point E of the link s that comes into contact with the sphere can be expressed as $\mathbf{v}_E = \mathbf{v}_{A_s} + \boldsymbol{\omega} \times \mathbf{r}_E$. The impact differential equation of motion for the slider-crank mechanism has two unknowns and to solve it another equation is needed. The second equation for the impact case can be written using Newton's coefficient of restitution e.

The velocity of approach can be written as $\mathbf{v}_a = [\mathbf{v}_E]_{t_1} - [\mathbf{v}_{\text{sphere}}]_{t_1}$ where $[\mathbf{v}_E]_{t_1}$ is the rod velocity at time t_1 before the impact and $[\mathbf{v}_{\text{sphere}}]_{t_1}$ is the sphere velocity at time t_1 before the impact.

The velocity of separation can be written as $\mathbf{v}_s = [\mathbf{v}_E]_{t_2} - [\mathbf{v}_{\text{sphere}}]_{t_2}$ where $[\mathbf{v}_E]_{t_2}$ is the rod velocity at time t_2 after the impact and $[\mathbf{v}_{\text{sphere}}]_{t_2}$ is the sphere velocity at time t_2 after the impact.

Thus, using Newton's formulation of the coefficient of restitution e, one can write the second equation of the system as

$$-e\mathbf{v}_a \cdot \mathbf{n} = \mathbf{v}_s \cdot \mathbf{n},$$

where $\mathbf{n}$ represents the normal to the rod.

3. Nonlinear dynamic analysis

Data obtained from a deterministic system can be classified as either periodic or non-periodic data [18]. Non-periodic data may correspond to a quasi-periodic, transient or chaotic motion. The term chaotic is assigned to those problems for which there are no random or unpredictable variable or parameters, but their time histories have a sensitive dependence on initial conditions. Thus, the motion is chaotic in the sense of not being predictable when there is a small uncertainty in the initial conditions. The chaotic motion is characterized by a continuous, broad-band Fourier spectrum and is possible only in a three-or-more dimensional nonlinear system of differential equations.

A set of equations represents a random system if any of the variables and/or parameters has a random character. If the data obtained from an experiment are not repeatable within the bounds of the experiment error under similar conditions, then the corresponding system can be called a random system. The data obtained from a random system is called random data.

The space defined by the independent coordinates required to describe a motion is called a state space (S), and the independent coordinates are called state variables. For a given system of equations, the coordinates of the state space are well defined. Considering a set of initial conditions, the time evolution of the system will describe trajectories in the state space. Depending on the parameters of the system, these trajectories can be divergent or convergent to a final state generally called attractor. In other words, an attractor is something that "attracts" initial conditions from a region around it once transients have died out. A more precise definition can be found in Farmer et al. [19]. Simple attractors can be: a system in equilibrium (point attractor), or those which decay into stable periodic states (limit cycles), or quasi-periodic motion. The chaotic evolution is associated with an attractor with the property that the system decays to a final state, but this state is not periodic and is extremely complex. This attractor is generally called strange attractor.

Lyapunov exponents provide a measure of the sensitivity of the system to its initial conditions. They exhibit the rate of divergence or convergence of the nearby trajectories from each other in state space and are fundamentally used to distinguish the chaotic and non-chaotic (periodic or quasi-periodic) behavior. Periodic attractors show only negative and zero exponents which indicate convergence to a predictable motion, whereas there exists at least one positive exponent for a chaotic system. Therefore, one needs to determine the sign of Lyapunov exponents to characterize the behavior of a dynamically system. For example, if one considers a 3D state space, so that there will be an exponent for each dimension, then all negative exponents will indicate the presence of a fixed point, one zero and the other negative a limit cycle, and one positive a chaotic attractor. It should be noted that an attractor exist only when the sum of all the Lyapunov exponents is negative.

The definition of Lyapunov exponents λ_i can be found in Wolf et al. [20] and the computation procedure in Kapitaniak [21].

The exponent measures the rate at which system processes create or destroy information. Thus, the exponents are expressed in bits of information.

We use the nonlinear technique of the Lyapunov exponents to evaluate the stability of the kinematic chain. One of the advantage of using this technique is the analysis could be performed by using experimentally acquired system states without having to build the equations of motion. The Lyapunov exponents provided a useful characterization of a given analytical or experimental data set, and are of importance to both the theoretical and the experimental understanding of dynamical systems.

4. Results

In this section, the dynamic evolution of the system is investigated. This consists in interconnected rigid and flexible components examined for different angular velocities. The slider-crank mechanism is driven by a prescribed torque profile, and periodically impacted, so that the motion is not known a priori, thus the differential equation of motion have been derived.

Numerical simulation for the slider-crank mechanism were performed for a particular system with a flexible link.

The flexible link has $n = 7$ successive equal rigid rods, each with the length 0.045 m. The link 1 has the length 0.12 m. For the rods, two kind of materials are chosen, steel and aluminum. The mass of the sphere is $m = 0.1$ kg. The coefficient of restitution is $e = 0.5$.

For the sphere simulations presented here an eight particle approximation ($q = 8$) was used. Simulations involving 9, 10, 11, 12 and 13 particles were performed and no perceptible difference was found with respect to the dynamic behavior. Thus $q = 8$ is considered adequate for accurately describing the elastic motion for the simulation reported in this paper.

For the mechanism simulations, a seven rigid rods approximation ($n = 7$ rigid links for the elastic rod) was used. Simulations involving 9, 11 and 15 rods were performed and no perceptible difference was found with respect to the dynamic behavior. Thus $n = 7$ was considered adequate for accurately describing the elastic motion of the mechanism for the simulation reported in this paper (Ref. [22]).

For the slider-crank mechanism, the horizontal coordinate x_{C_5}, of the mass center of link 5 was analyzed. The motion (trajectory of the mass center of link 5) on x-axis of the slider-crank mechanism without impacts was shown (refer to Fig. 4a). In the same figure, the trajectory of the mass center of link 5 with impact was presented. The mechanism changes its trajectory after the moment of impact at $t = 0.004$ s. The thicker curve in the figure is related to the trajectory of the mechanism with impact.

The trajectories of the sphere with and without impact are presented in Fig. 4b, and the trajectory of the vertical coordinate y_{G_s}, of the mass center of the sphere was drawn. The thicker curve in the figure is related to the trajectory of the sphere with impact.

Next, the vertical coordinate of the mass center of the link 5 is analyzed.

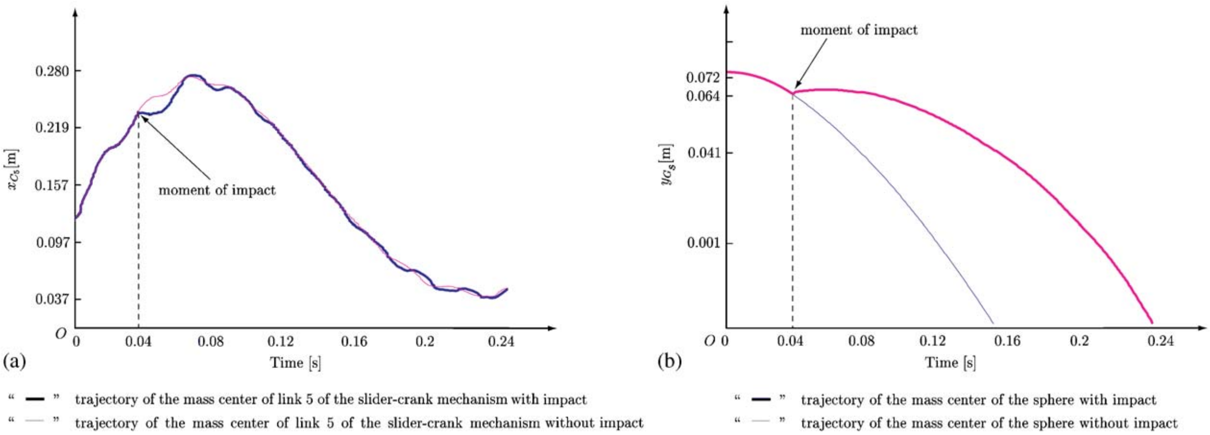

Fig. 4. Trajectory of the mass center of the sphere and slider-crank mechanism: (a) of the Link 5 of the slider-crank mechanism with and without impact, (b) of the vertical coordinate of the mass center of the sphere with and without impact.

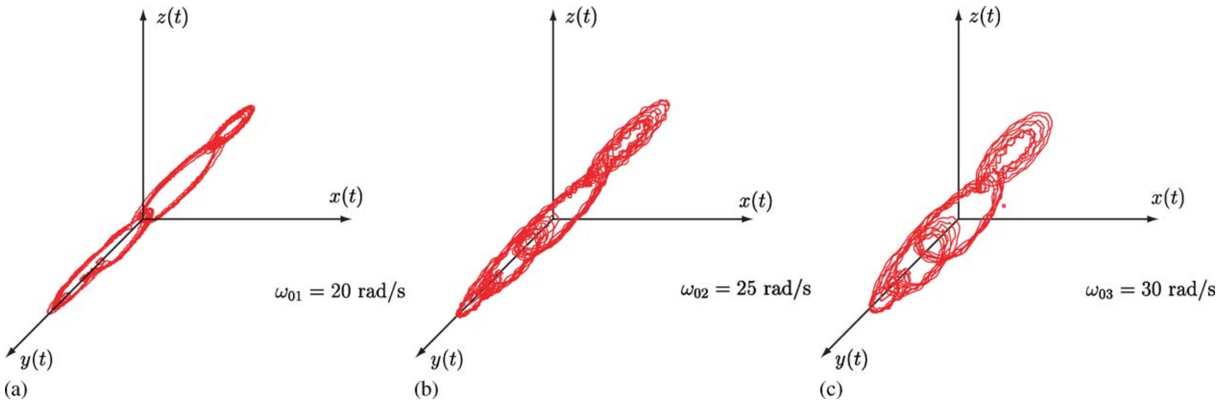

Fig. 5. 3D phase space generated by the system evolution for aluminum specimen for different angular velocities $\omega_{01} = 25$, $\omega_{02} = 30$ and $\omega_{03} = 35\,\text{rad/s}$.

Fig. 5 shows the 3D phase space generated by the system evolution for aluminum for different angular velocities $\omega_{01} = 25$, $\omega_{02} = 30$ and $\omega_{03} = 35\,\text{rad/s}$. Fig. 6 shows the 3D phase space generated by the system evolution for steel at the same angular velocities $\omega_{01} = 25$, $\omega_{02} = 30$ and $\omega_{03} = 35\,\text{rad/s}$. The trajectory shown in Figs. 5 and 6 for each particular specimen, steel or aluminum, are associated with the motion around the attractor and shows the classical characteristics of chaotic motion. It is visible in all cases that the phase trajectory of the link 5 vibration does not close for each revolution.

The type of dynamical evolution of the system is best shown by the sign of the largest Lyapunov exponent.

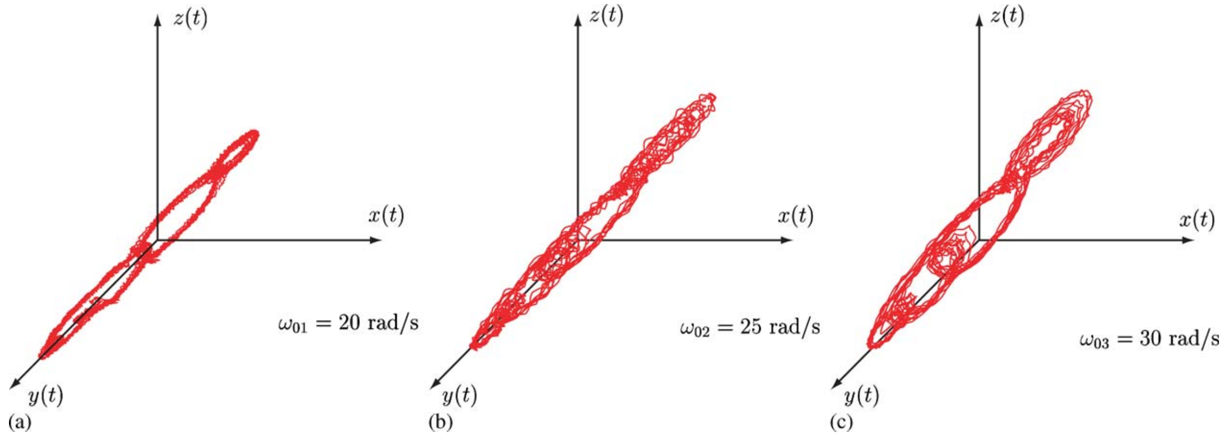

Fig. 6. 3D phase space generated by the system evolution for steel specimen for the angular velocities $\omega_{01} = 25$, $\omega_{02} = 30$ and $\omega_{03} = 35\,\text{rad/s}$.

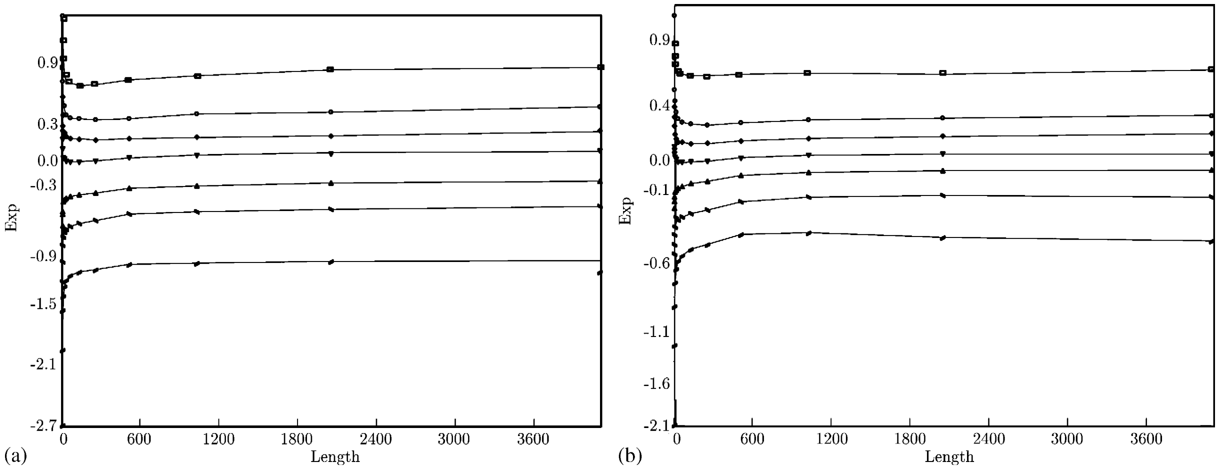

Fig. 7. Local Lyapunov exponents: (a) for the aluminum specimen, (b) for steel specimen.

Fig. 7a shows all computed Lyapunov exponents for aluminum when $\omega_0 = 35\,\text{rad/s}$. Fig. 7b shows all computed Lyapunov exponents for steel at the same angular velocity $\omega_0 = 35\,\text{rad/s}$.

For both cases, aluminum and steel, one Lyapunov exponent is zero, thus, the systems can be described by a dynamical system of differential equations. The sign of the largest Lyapunov exponents is positive for all data (aluminum or steel specimens), denoting the exponential separation of nearby trajectories as time evolves, that is, the system is characterized by chaotic behavior. So, one can conclude at this point the chaotic behavior of each system.

For aluminum, the largest Lyapunov exponents λ_{ia} have been computed for different angular velocities $\omega_{01} = 25$, $\omega_{02} = 30$ and $\omega_{03} = 35\,\text{rad/s}$. The values of the largest Lyapunov exponents are $\lambda_{1s} = 0.4$ to the corresponding $\omega_{01} = 25\,\text{rad/s}$, $\lambda_{2s} = 0.67$ to the corresponding $\omega_{02} = 30\,\text{rad/s}$ and $\lambda_{3s} = 0.91$ to the corresponding $\omega_{03} = 35\,\text{rad/s}$.

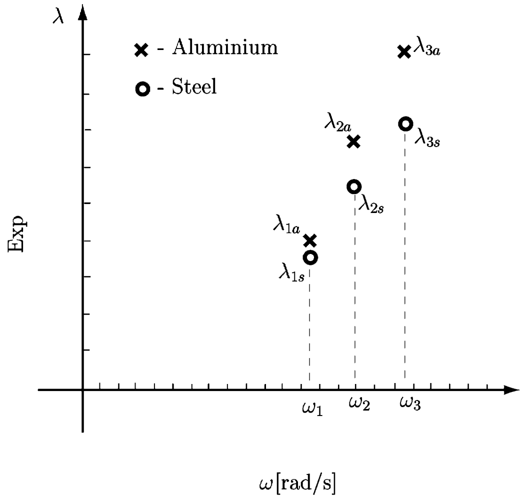

Fig. 8. Largest Lyapunov exponents for aluminum specimen λ_{1a}, λ_{2a}, λ_{3a} and for steel specimen λ_{1s}, λ_{2s}, λ_{3s}.

For steel, the largest Lyapunov exponents λ_{is} have been computed for the same angular velocities ω_{01}, ω_{02} and ω_{03} as in the aluminum case. The values of the largest Lyapunov exponents are $\lambda_{1a} = 0.36$ to the corresponding $\omega_{01} = 25\,\text{rad/s}$, $\lambda_{2a} = 0.54$ to the corresponding $\omega_{02} = 30\,\text{rad/s}$ and $\lambda_{3a} = 0.74$ to the corresponding $\omega_{03} = 35\,\text{rad/s}$.

In Fig. 8 the largest Lyapunov exponents λ_{1a}, λ_{2a}, λ_{3a} for the aluminum case and λ_{1s}, λ_{2s}, λ_{3s} for the steel case with respect to the angular velocities $\omega_{01} = 25$, $\omega_{02} = 30$ and $\omega_{03} = 35\,\text{rad/s}$ are shown. One can see an increase in values of Lyapunov exponents as the angular velocity increases. These increase appear also in steel or aluminum case. Also, one can observe that for the same angular velocity the Lyapunov exponents for aluminum are greater than the Lyapunov exponents for steel, that is, $\lambda_{ia} > \lambda_{is}$.

5. Conclusions

In this paper the motion of a slider-crank mechanism with impact and a flexible component was analyzed. Using Lyapunov exponents the stability of the system is investigated and one can observe that the system is chaotic. The existence of chaotic vibrations is confirmed in both cases, steel or aluminum. One can see an increase in values of Lyapunov exponents as the angular velocity increases, that is, when $\omega_{01} > \omega_{02} \Rightarrow \lambda_1 > \lambda_2$. Also one can observe that for the same angular velocity ω_{0i} =const. $\Rightarrow \lambda_{ia} > \lambda_{is}$. Furthermore, experimental tests with different materials are needed in order to generalize the results reported in the present paper.

References

[1] Y.A. Khulief, A.A. Shabana, Impact responses of multi-body system with consistent and lumped masses, *Journal of Sound and Vibration* 104 (2) (1986) 187–207.

[2] A. Mioduchowski, M. Faulkner, A. Pielorz, W. Nadolski, Longitudinal collision of rod-rigid elements systems, *Journal of Applied Mechanics* 50 (1983) 59–69.
[3] V. Feliu, K.S. Rattan, H.B. Brown, Modeling and control of single-link flexible arms with lumped masses, *Journal of Dynamic Systems Measurement and Control* 114 (1992) 59–69.
[4] D. Rubinstein, Dynamics of a flexible beam and a system of rigid rods, with fully inverse (one-sided) boundary conditions, *Computers and Methods in Applied Mechanical Engineering* 175 (1999) 87–97.
[5] S.W. Shaw, R.H. Rand, The transition to chaos in a simple mechanical system, *International Journal of Non-linear Mechanics* 24 (1) (1989) 41–56.
[6] F.C. Moon, S.W. Shaw, Chaotic vibrations of a beam with non-linear boundary conditions, *International Journal of Non-linear Mechanics* 18 (6) (1983) 465–477.
[7] S.W. Shaw, The dynamics of a harmonically excited system having rigid amplitude constraints—Part 1,2, *Journal of Applied Mechanics* 52 (2) (1985) 453–464.
[8] S. Dubowsky, M. Moening, An experimental and analytical study of impact forces in elastic mechanical system with clearances, *Mechanism and Machine Theory* 64 (1978) 89–95.
[9] D.B. Moore, S.W. Shaw, The experimental response of impact pendulum system, *International Journal of Non-linear Mechanics* 25 (1) (1990) 1–16.
[10] J. Shaw, S.W. Shaw, The onset of chaos in a two-degree-freedom impact system, *Journal of Applied Mechanics* 56 (1989) 168–174.
[11] L.D. Seneviratne, S.W.E. Earles, Chaotic behavior exhibited during contact loss in a clearance joint of a four-bar mechanism, *Mechanism and Machine Theory* 27 (3) (1992) 307–321.
[12] F. Farahanchi, S.W. Shaw, Chaotic and periodic dynamics of a slider-crank mechanism with slider clearance, *Journal of Sound and Vibration* 177 (3) (1994) 307–324.
[13] P. Szuminski, T. Kapitaniak, Stability regions of periodic trajectories of the manipulator motion, *Chaos, Solitons and Fractals* 17 (2003) 67–78.
[14] D.B. Marghitu, Y. Hurmuzlu, Three-dimensional rigid-body collisions with multiple contact points, *Journal of Applied Mechanics* 62 (1995) 725–732.
[15] M. Dupac, D.G. Beale, D.B. Marghitu, Lumped mass modelling and chaotic behavior of an elastic levitated droplet, *Nonlinear Dynamics* 27 (2002) 311–326.
[16] D. Stoianovici, Y. Hurmuzlu, A critical study of the concepts of rigid body collision theory, *Journal of Applied Mechanics* 63 (1996) 307–316.
[17] R.J. Roark, W.C. Young, *Formulas for Stress and Strain*, McGraw-Hill, New York, 1975.
[18] A.H. Nayfeh, B. Balachandran, *Applied Nonlinear Dynamics*, Wiley, New York, 1995.
[19] J.D. Farmer, E. Ott, J.A. Yorke, The dimension of chaotic attractors, *Physica D* 7 (1983) 153–180.
[20] A. Wolf, J.B. Swift, H.L. Swinney, J.A. Vastano, Determining Lyapunov exponents from a time series, *Physica D* 16 (1985) 285–317.
[21] T. Kapitaniak, *Chaotic Oscillations in Mechanical Systems*, Manchester University Press, Manchester, 1991.
[22] D.B. Marghitu, Y. Hurmuzlu, Nonlinear dynamics of an elastic rod with frictional impact, *International Journal of Nonlinear Dynamics* 10 (1996) 187–201.